 doi:10.20944/preprints202112.0037.v1

Article

Optimal relay network for aerial remote inspections

Luis Pinto [1], Luis Almeida [2,*]

[1] independent researcher; eng.pintoluis@gmail.com
[2] CISTER, Faculdade de Engenharia da Universidade do Porto, Porto, Portugal; lda@fe.up.pt
* Correspondence: lda@fe.up.pt;

Abstract: Unmanned Aerial Vehicles (UAVs) in particular multirotors are becoming the *de facto* tool for aerial sensing and remote inspection. In large industrial facilities, a UAV can transmit an online video stream to inspect difficult to access structures, such chimneys, deposits and towers. However, the communication range is limited, constraining the UAV operation range. This limitation can be overcome with relaying UAVs placed between the source UAV and the control station, creating a line of communication links. In this work we assume the use of a digital data packet network technology, namely WiFi, and tackle the problem of defining the exact placement for the relaying UAVs that creates an end-to-end channel with maximal delivery of data packets. We consider asymmetric communication links and we show an increase as large as 15% in end-to-end packet delivery ratio when compared to an equidistant placement. We also discuss the deployment of such a network and propose a fully distributed method that converges to the global optimal relay positions taking, on average, 1.4 the time taken by a centralized method.

Keywords: Multi-hop network, packet delivery ratio, relay network, TDMA, throughput, UAV, wireless networks

1. Introduction

The versatility of Unmanned Aerial Vehicles (UAV or *drones*) has allowed their use for multiple purposes, either recreational, engineering, scientific or military. Many of these applications require remote vision, either for their own control with First-Person-View (FPV), for aerial sensing of areas of interest or for remote inspection of large structures that are difficult to access. This last case can be found in widespread industrial plants to inspect chimneys, silos, reactors, buildings, etc [1]. In these situations, an UAV typically captures a video stream that is transmitted to an operator in a base station that fine tunes the navigation and positioning of the UAV to carry out the inspection with detail. Multirotor UAVs are particularly suited to such situations because of their high maneuverability, including hovering capacity, and ad-hoc communication that dispenses a pre-deployed network infrastructure. However, the wireless transmission from the UAV to the base station poses a limit to the device range of operation. This is particularly relevant when using data networks, such as IEEE 802.11 (WiFi), which may improve the quality of the video transmission, and integrate other data communications, too, but exhibit abrupt degradation with distance.

One possible way to mitigate the range limitation is adding UAV relays that can hover between the source UAV and the base station, forwarding packets from one side to the other, forming a multi-hop line network (Figure 1). This kind of network was studied in [2] with a characterization of the end-to-end communication channel as a function of the properties of the individual links, namely the end-to-end throughput as a function of the links Packet Delivery Ratio (PDR). The authors proposed and validated in practice a model for the link PDR degradation with distance. With such model they showed how to place the relays optimally to cover the largest distance with the minimum number of relays, while simultaneously maximizing the end-to-end throughput. Minimizing the number of UAVs is particularly relevant because it allows reducing end-to-end latency,

Preprints (www.preprints.org) | NOT PEER-REVIEWED | Posted: 2 December 2021 doi:10.20944/preprints202112.0037.v1

which is crucial in the use cases we are considering. In practice, we do not envisage networks with more than just a few relays, hardly above 5 or 6.

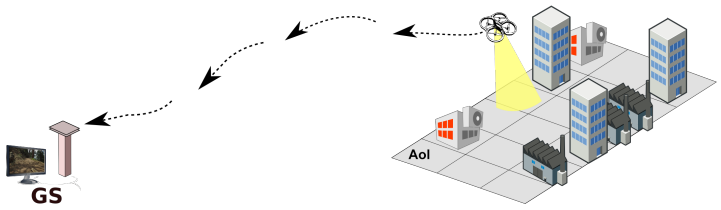

Figure 1. Single-source aerial stream to a ground sink using UAV relays to transmit data.

The previous work considered links with similar PDR model, each transmitting within an exclusive time slot of a Time-Division Multiple-Access (TDMA) scheme. In such conditions, the optimal relay placement is equidistant along the source to base station path. However, the assumption of links with similar PDR model falls short in practice, since the links often exhibit asymmetric properties due to obstacles, differences in the antennas, local interference, among other effects. These link asymmetries cause different error rates and throughput, negatively impacting the network end-to-end features. This was shown in [3], where the authors proposed a method to compensate those asymmetries acting on the throughput, adjusting the duration of the time slots so to give less time to links that have high throughput and vice-versa. This provides a fast compensation method for a network with asymmetric but fixed link properties, balancing the throughput among all network links.

A better asymptotic result can be achieved by adapting the position of the relays dynamically to balance the link PDR instead of the throughput. The work in [4] shows a preliminary incursion in this direction, analyzing the case of one relay, determining the optimal relay placement between a fixed source and base station, and validating this result in practice. However, no formal method to solve the optimization problem was shown, just empirical solutions. Here, we follow the same line of research, complementing the previous work by addressing the general case of a line network with n links between a source node (the source UAV) and a sink (the base station), constrained to a total fixed length C, with each link characterized by an empirical PDR quality model. We provide the optimal solution to the relay placement problem that balances the links properties and maximizes the end-to-end PDR. We also consider that the Medium Access Control (MAC) layer uses a TDMA transmission control scheme to prevent transmission collisions, automatic retries are disabled and the bit rate is fixed. Under these assumptions, the end-to-end throughput can also be directly derived from the end-to-end PDR.

Our contributions are the following:

- An optimal (global) solution for relay placement considering asymmetric links. This work subsumes the work in [2] that considered symmetric links, but builds on the empirical link PDR models developed therein.
- Two deployment strategies with centralized and distributed positions control. We provide a comparison between both in terms of convergence time and overhead, together with an empirical proof of convergence of the distributed solution to the global optimal relay positions.

The next section discusses related work available in the literature. Section 3 introduces the problem of relaying video over a line of hovering relays and shows the formal grounds for the asymmetric relay placement. Section 4 presents the optimal relay placement solution, with examples and performance assessment. Section 5 presents two deployment methods for the solution proposed before, namely a centralized and a distributed relay positions control methods. Emphasis is made on the distributed method, its relative performance and convergence. The online estimation of the links PDR model is also introduced. Finally, Section 6 concludes the paper.

Preprints (www.preprints.org) | NOT PEER-REVIEWED | Posted: 2 December 2021 doi:10.20944/preprints202112.0037.v1

2. Related Work

Using UAVs as flying sensors has already been extensively studied for multiple purposes, either commercial, military and research, especially for image/video sensing and its applications. For example, the works in [5,6] rely on UAVs to carry out SLAM (simultaneous localization and mapping) from cameras and LiDAR to obtain 3D maps of the scenario. Other works address the wireless communication and the associated network of UAVs. The work in [7] focuses on the wireless link with a UAV, using IEEE 802.11g and UDP/IP, and the impact of using different PHY bit-rates, inter-node distances and relative velocities. Extensive experimental results focusing on throughput show a positive impact of setting the bit-rate manually. Conversely, the work in [8] shows that when multiple UAVs carry out simultaneous video streaming over the wireless network, the overall performance is improved by having the multiple transmitters adapt their PHY bit-rate as a function of the network load and link conditions. The work in [9] goes one step further in discussing how to set up a sensor network using UAVs, considering scenarios in which sensors can be temporarily disconnected, when the sensors are all within range of a base station and connect directly to it, and when relays are added to extend the range of communication. Further performance improvements of wireless multi-hop communication require acting at the network management level, from routing, using specific protocols such as AODV, DSDV, BATMAN and their variants, to traffic control with shapers, including TDMA, leaky buckets and other, and/or using redundancy to mitigate the typical unreliability of the wireless links.

One important observation is that the approaches referred above either consider uncontrollable or fixed nodes, particularly not exploring the movement of nodes for the sake of improving some network features. Some other works addressed the dynamic behavior of certain network features, such as the PDR, under mobility [10,11], but considering low throughput scenarios. In such a case, overflows of internal network buffers, which are a major source of packet losses under high throughput, are not necessarily a problem, dispensing the use of traffic throttling mechanisms. A complementary work [12] addressed the case of data streaming in a vehicular network, looking into the impact of relative speed on PDR, but considering single hop communication, only.

Another related research line is that of robotic networks of ground, or surface, autonomous mobile robots. One work that marked this line is that in [13], where the authors investigate controlling the movement of one robot that transmits wirelessly a data stream to a base station, possibly over a multi-hop network. Instead of transmitting and moving at a constant pace along the way, the authors propose slowing the robot whenever the channel is good while accelerating the robot motion whenever the channel exhibits poor characteristics. This effectively results in a spatial asymmetry of transmissions, concentrating them in spots of good connectivity, and in an increase of the average throughput for streaming data over a multi-hop network. The work in [14] addresses another very relevant topic in mobile robotic networks performance. It shows a characterization of the network performance when varying the distance from a base station and with different data-rate and delay user requirements. However, they propose adopting a data mule model when the robots move farther away from the base station, using delay tolerant networking, instead of online relaying. In these conditions, PDR assume less relevance and the authors to not address it. Finally, the works in [15] and [16] are probably those that exhibit the highest relevance to work work since they also aim at setting up a line of relay nodes to convey a multimedia stream from a source robot in one extreme to a base station on the other. However, beyond using ground robots, these works address the specific features of wireless communication within tunnels and pipelines, such as the wave-guide-like behavior, which is very specific to such scenarios.

Looking at all these works, despite being close to our work topic-wise in different aspects, to the best of our knowledge, no previous work addressed the case of controlling dynamically the position of flying hovering UAV nodes to set up a line of relays that provides a WiFi communication channel with maximal end-to-end PDR to a source UAV

Preprints (www.preprints.org) | NOT PEER-REVIEWED | Posted: 2 December 2021 doi:10.20944/preprints202112.0037.v1

that transmits a bandwidth-intensive live video stream to a base station. This is the problem we address in this work and which we formalize in the following section.

3. Problem

As referred previously, in this work we consider an aerial network of n UAVs with hovering capacity, such as multirotors, identified uniquely by their index $i \in [1, n]$, and a ground (or control) station with index $i = 0$. The UAVs form a line network topology and communicate essentially in one direction, only, from the farthest (1^{st}) UAV, which we call the source that generates a live sensing (video) stream, to the ground station, which we will call sink[1]. We assume that all intermediate UAVs ($i \in [2, n]$) are relays that communicate with their immediate neighbors, only. This implies the existence of n links, i.e., node i receives the sensing stream from node $i-1$ through link $i-1$ and retransmits it to node i through link i. Finally, we consider the links to be physically aligned[2] with a total network length of L. Figure 2 shows an example with n UAVs and a sink (in blue), in which the 1^{st} UAV is the source (in pink) and UAVs 2 to n are relays. There are n links with lengths d_1 to d_n, with a total network length of $L = d_1 + d_2 + \cdots + d_n$.

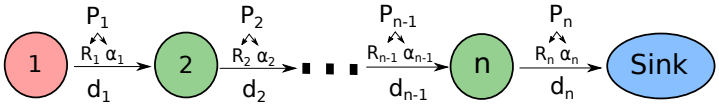

Figure 2. Multi-hop line network model. The PDR of link i, between nodes i and $i+1$, is P_i with parameters R_i, α_i, and its length is d_i.

In what concerns the Packet Delivery Ratio (PDR) of each link, we use the model proposed in [2] in which a link i exhibits a PDR P_i that varies with the link length d_i according to a negative exponential law as presented in Eq. 1. Here, β_i is given by Eq. 2, R_i is the link length at which the PDR is reduced to 50% and α_i is related to the slope of the PDR curve at length R. Along the formal developments that follow, we will frequently refer to link i as its corresponding PDR model duplet (R_i, α_i).

$$P_i(d_i) = e^{\beta_i \, {d_i}^{\alpha_i}} \tag{1}$$

$$\beta_i = \frac{-\log(2)}{{R_i}^{\alpha_i}} \tag{2}$$

Once the network model and link PDR model are defined, we can now formalize the problem at hand. In this work our objective is to maximize the performance of the line network in what concerns the end-to-end PDR by adjusting the placement of the relay nodes along the line, or equivalently, adjusting the lengths of the network links subject to the total fixed network length L. Before we express this objective formally, it is important to state a few more assumptions. First, we assume that packets lost in the forwarding process are not recovered. If relevant, recovery must be managed at a higher layer. This is common with streams of real-time data as is the case, here. Moreover, we consider that the processes that generate packet losses are independent across links. This also means that the performance of each link i is solely dependent on its length d_i and the medium characteristics (R_i, α_i), being all links independent of each other. Finally, we assume there is a global TDMA coordination scheme in place, so that nodes transmit in their disjoint time slots, only, preventing interference among nodes transmissions.

[1] Although we consider unidirectional source to sink communication, only, our model does not preclude low-bandwidth communication in the opposite direction, such as controls sent by the ground station to the UAVs. Note that the corresponding bandwidth is significantly lower than that of the online sensing stream, reducing the relevance of PDR optimization in that direction since reliable retransmission-based mechanisms can be put in place. Thus, for our work we ignore other than the source to sink transmissions.

[2] The constraint of physical alignment is currently relevant, since we consider that, when moving one relay, one of its links shrinks while the other one grows the same length, given the fixed total length. The case of links that can form different angles between them is left for future work.

Preprints (www.preprints.org) | NOT PEER-REVIEWED | Posted: 2 December 2021 doi:10.20944/preprints202112.0037.v1

Under these assumptions, the end-to-end PDR can be obtained by a simple multiplication of the PDRs of the individual links, as expressed in Eq. 3. Here we use $\mathbf{d}$ to represent the vector of n link lengths and $P_{\texttt{net}}(\mathbf{d})$ as the end-to-end network PDR that results from applying the link lengths vector $\mathbf{d}$.

$$\begin{aligned} P_{\texttt{net}}(\mathbf{d}) &= \prod_{i=1}^{n} P_i(d_i) \\ \mathbf{d} &= [d_1, d_2, d_3, ..., d_n] \end{aligned} \tag{3}$$

We can now state our optimization problem as in Eq. 4, i.e., finding the vector of link lengths $\mathbf{d}$ that maximizes the end-to-end PDR $P_{\texttt{net}}(\mathbf{d})$, subject to the fixed network length constraint L.

$$\begin{aligned} P_{\texttt{opt}} = \max_{\mathbf{d}} P_{\texttt{net}}(\mathbf{d}) = \max_{\mathbf{d}} \prod_{i=1}^{n} P_i(d_i) = e^{\beta_1 {d_1}^{\alpha_1}} \cdot ... \cdot e^{\beta_n {d_n}^{\alpha_n}} \\ \text{st. } L - \sum_{k=1}^{n} d_k = 0 \end{aligned} \tag{4}$$

4. Global Solution

To solve the optimization problem expressed in Eq. 4 we resort to the Lagrangian method for maximization. Thus, we start by expressing the corresponding Lagrangian expression $\mathcal{A}(\mathbf{d})$ as in Eq. 5 and its gradient as in Eq. 6.

$$\mathcal{A}(\mathbf{d}) = \prod_{i=1}^{n} P_i(d_i) + \lambda \left(L - \sum_{i=1}^{n} d_i \right) \tag{5}$$

$$\nabla_{d_1, d_2, ..., \lambda} = \left(\frac{\partial \mathcal{A}}{\partial d_1}, ..., \frac{\partial \mathcal{A}}{\partial \lambda} \right) \tag{6}$$

To solve the gradient, we start by computing the partial derivatives of the Lagrangian expression with respect to d_i, as in Eq. 7.

$$\frac{\partial}{\partial d_i} \mathcal{A}(\mathbf{d}) = \left(\prod_{j=1, j \neq i}^{n} P_j(d_j) \right) \cdot \frac{d}{d d_i} P_i(d_i) - \lambda \tag{7}$$

Note that deriving $P_i(d_i)$ is straightforward since it is an exponential function, resulting in Eq. 8. Thus, we can now rewrite Eq. 7 as in Eq. 9.

$$\begin{aligned} \frac{d}{d d_i} P_i &= \frac{d}{d d_i} e^{\beta_i {d_i}^{\alpha_i}} = \\ &= \left(\frac{d}{d d_i} \beta_i {d_i}^{\alpha_i} \right) e^{\beta_i {d_i}^{\alpha_i}} = \left(\beta_i \alpha_i {d_i}^{\alpha_i - 1} \right) P_i \end{aligned} \tag{8}$$

$$\frac{\partial}{\partial d_i} \mathcal{A}(\mathbf{d}) = \left(\prod_{j=1, j \neq i}^{n} P_j(d_j) \right) \cdot \left(\beta_i \alpha_i {d_i}^{\alpha_i - 1} \right) P_i - \lambda \tag{9}$$

We can now establish the gradient of $\mathcal{A}(\mathbf{L})$ as in Eq. 10.

Preprints (www.preprints.org) | NOT PEER-REVIEWED | Posted: 2 December 2021 doi:10.20944/preprints202112.0037.v1

$$\nabla_{d_i \forall_{i\in[1,n]},\lambda} = \left(\forall_{i\in[1,n]}\left[\left(\beta_i\alpha_i {d_i}^{\alpha_i-1}\right)\prod_{k=1}^{n} P_k(d_k) - \lambda\right], L - \sum_{k=1}^{n} d_k\right) \tag{10}$$

To solve the maximization problem, we equal the gradient to zero and solve for d_i, thus obtaining the following system of equations (Eq. 11):

$$\begin{aligned} &\nabla_{d_1,d_2,\ldots,\lambda} = 0 \Leftrightarrow \\ \Leftrightarrow &\begin{cases} \beta_1\alpha_1 {d_1}^{\alpha_1-1}\prod_{k=1}^{n} P_k(d_k) - \lambda = 0 \\ \beta_2\alpha_2 {d_2}^{\alpha_2-1}\prod_{k=1}^{n} P_k(d_k) - \lambda = 0 \\ \ldots \\ \beta_n\alpha_n {d_n}^{\alpha_n-1}\prod_{k=1}^{n} P_k(d_k) - \lambda = 0 \\ L - \sum_{k=1}^{n} d_k = 0 \end{cases} \end{aligned} \tag{11}$$

This system of equations also means that, for any two nodes g and h, we have the following relationship (Eq. 12):

$$\begin{aligned} & \beta_g\alpha_g {d_g}^{(\alpha_g-1)} = \beta_h\alpha_h {d_h}^{(\alpha_h-1)} & \Leftrightarrow \\ \Leftrightarrow \quad & {d_g}^{(\alpha_g-1)} = \frac{\beta_h\alpha_h}{\beta_g\alpha_g} {d_h}^{(\alpha_h-1)} & \Leftrightarrow \\ \Leftrightarrow \quad & d_g = \left(\frac{\beta_h\alpha_h}{\beta_g\alpha_g}\right)^{\left(\frac{1}{\alpha_g-1}\right)} d_h^{\left(\frac{\alpha_h-1}{\alpha_g-1}\right)} \end{aligned} \tag{12}$$

Considering that most of the terms in Eq. 12 correspond to constants, we can thus rewrite the optimal links length relationship as in Eq. 13.

$$\begin{aligned} & d_g = \Psi_{g,h} \cdot {d_h}^{\theta_{g,h}} \\ & \text{where:} \\ & \Psi_{g,h} \equiv \left(\frac{\beta_h\alpha_h}{\beta_g\alpha_g}\right)^{\left(\frac{1}{\alpha_g-1}\right)} = \left(\frac{{R_g}^{\alpha_g}\alpha_h}{{R_h}^{\alpha_h}\alpha_g}\right)^{\left(\frac{1}{\alpha_g-1}\right)} \\ & \theta_{g,h} \equiv \left(\frac{\alpha_h-1}{\alpha_g-1}\right) \end{aligned} \tag{13}$$

In practical terms, to solve the system in Eq. 11 we can start by computing d_n first and then use the ratio in Eq. 13 to express all other d_i with $i \in [1, n-1]$ as a function of d_n. This is expressed in Eq. 14.

$$\begin{cases} d_1 = \Psi_{1,n} \cdot {d_n}^{\theta_{1,n}} \\ d_2 = \Psi_{2,n} \cdot {d_n}^{\theta_{2,n}} \\ \ldots \\ d_{n-1} = \Psi_{n-1,n} \cdot {d_n}^{\theta_{n-1,n}} \\ L = d_1 + d_2 + \ldots + d_n \end{cases} \tag{14}$$

To compute d_n we can take the last equation in the system and rewrite it as a function of d_n, only (Eq. 15).

$$L = \sum_{i=1}^{n-1}\left(\Psi_{i,n} \cdot d_n^{\theta_{i,n}}\right) + d_n \tag{15}$$

Preprints (www.preprints.org) | NOT PEER-REVIEWED | Posted: 2 December 2021 doi:10.20944/preprints202112.0037.v1

Nevertheless, in the general case, Eq. 15 has no closed-form expression. It is a Laurent polynomial, i.e., a polynomial with fractional (and/or negative) exponents, and the most common way of solving such polynomials is resorting to numerical methods such as a binary search. That is the approach followed in this work.

Finally, note that if the link PDR models are equal, then constants $\Psi_{g,h} = \theta_{g,h} = 1, \forall_{g.h}$, which implies, from Eq. 11, that the optimal network PDR (end-to-end) is achieved when all links have the same length, i.e, the relays are placed equidistantly between source and sink. This matches the results in [2], which are subsumed in our current work.

4.1. Examples

To illustrate the problem and solution method we just described, we herein present two examples, one with two links, thus source, sink and one relay in between, and another one with three links, thus with two relays in between. We will consider that the link models are known for all links, an assumption that will be dropped later on. The parameters of the link model were obtained randomly within ranges that were observed in practice, to preserve material consistency.

4.1.1. A case with two links

Consider a set of two links ($n = 2$) defined by models $\{(R_i, \alpha_i), i \in [1,2]\}$ with vectors $R = [100, 120]$ and $\alpha = [2.6, 2.6]$, and total network length $L = 140m$. We thus aim at finding the set of link lengths $\mathbf{d} = [d_1, d_2]$ that maximizes the end-to-end PDR $P_{\mathtt{net}}(\mathbf{d}) = \prod_{i=1}^{2} P_i(d_i)$, keeping L constant, as stated in Eq. 4.

We start by computing the constant vectors Ψ and θ as in Eq. 13:

$$\Psi_{1,2} = \left(\frac{100^{2.6}}{120^{2.6}}\right)^{1/1.6} = 0.7436$$
$$\theta_{1,2} = 1$$

Then, we compute d_n (in this case d_2) as a solution for the Laurent polynomial presented in Eq. 15.

$$\Psi_{1,2}\, {d_2}^{\theta_{1,2}} + d_2 = \Psi_{1,2}\, d_2 + d_2 = L \Leftrightarrow$$
$$d_2 = L/(1 + \Psi_{1,2}) \approx 80.3$$

Knowing the optimal length of second link (d_2), we can, in this simple case, directly extract the optimal length of the first link (d_1) from the network length constraint L.

$$d_1 = L - d_2 \approx 59.7$$

The maximal end-to-end PDR $P_{\mathtt{net}}$ that can be achieved with the referred links occurs when the link lengths are $\mathbf{d}_{opt} = [59.7, 80.3]m$ and its value is the following:

$$P_{\mathtt{opt}} = P_{\mathtt{net}}(\mathbf{d}_{\mathtt{opt}}) = P_1(59.7) \cdot P_2(80.3) = 0.6536$$

Generally, with n links we can represent the PDR solution in an n-dimensional graph. Thus, in this case, we can illustrate it with a 2D plot (Figure 3). The figure shows the PDR of the network (indicated as "product") and of both links as a function of the position of the relay with respect to the source node, i.e., the length of the first link. The network length, $L = d_1 + d_2$, is the position of the source, considered fixed. The network PDR has a maximum at $d_1 = 59.7$m, contradicting, for example, the intuition that it would be maximized at the point that equalizes the links PDR ($\sim$63m).

Preprints (www.preprints.org) | NOT PEER-REVIEWED | Posted: 2 December 2021 doi:10.20944/preprints202112.0037.v1

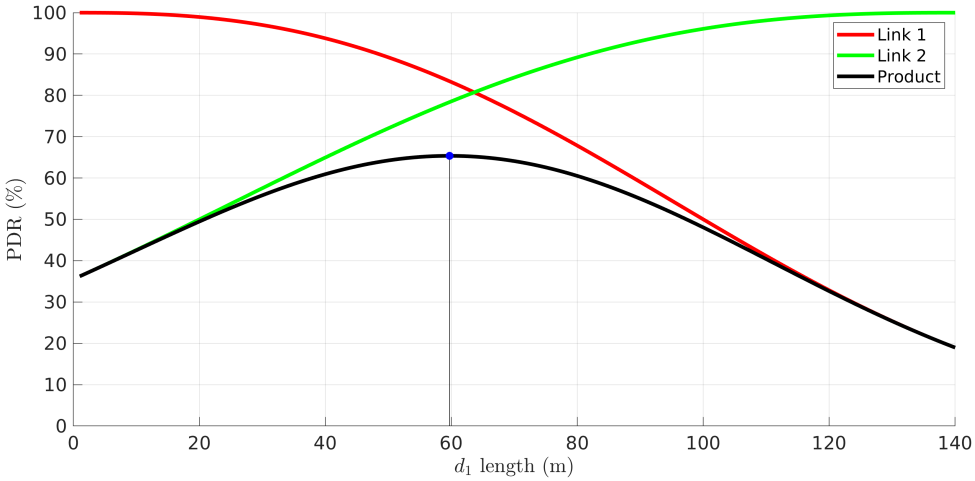

Figure 3. PDR of link 1 (red), link 2 (green) and their product, i.e., network (black), as a function of the length of the first link d_1 and $L = 140$.

4.1.2. A case with three links (two relays)

To show a case that already bears some more complexity, we present here a situation with three links, thus using two relays. The problem is as follows. Consider a set of three links ($n = 3$) defined by models $\{(R_i, \alpha_i), i \in [1,3]\}$ with vectors $R = [110, 120, 130]$ and $\alpha = [2.1, 3.2, 4.2]$, and total network length $L = 180m$. We now aim at finding the set of link lengths $\mathbf{d} = [d_1, d_2, d_3]$ that maximizes the end-to-end PDR $P(\mathbf{L}) = \prod_{i=1}^{3} P_i(d_i)$, keeping L constant (Eq. 4).

Figure 4 represents the PDR curves of the three links. Note that, in this case, we cannot represent symmetrically the pairs of PDR curves of the two links used by each relay, as in Figure 3, since we lack one fixed node in either case; relay 1 lacks a fixed node on the right side link and relay 2 lacks a fixed node on the left side link.

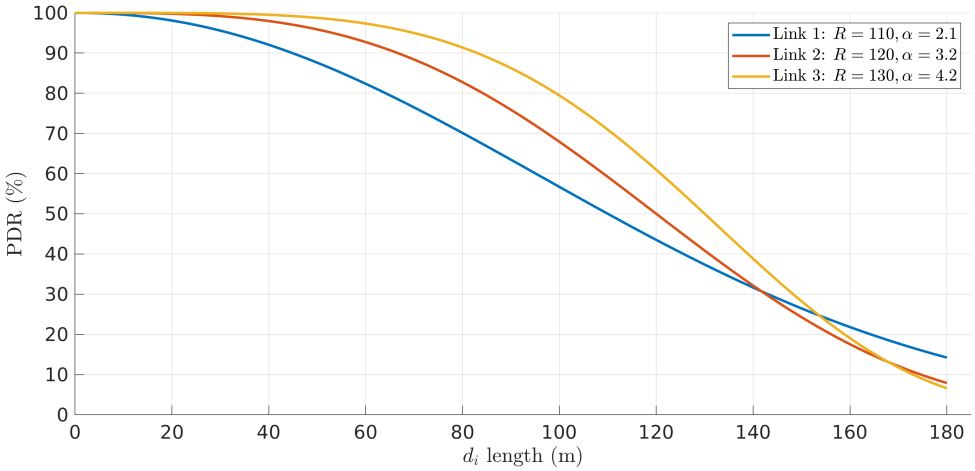

Figure 4. PDR of link 1, link 2 and link 3 as a function of their length.

Again, we start by computing the constant vectors Ψ and θ:

$$\Psi_{1,3} = 0.000126 \qquad \Psi_{2,3} = 0.1102$$
$$\theta_{1,3} = 0.110214 \qquad \theta_{2,3} = 1.4545$$

Then, we compute the solution of the corresponding Laurent polynomial (Eq. 15):

$$\left(\Psi_{1,3} \cdot d_3^{\theta_{1,3}}\right) + \left(\Psi_{2,3} \cdot d_3^{\theta_{2,3}}\right) + d_3 = L$$

Preprints (www.preprints.org) | NOT PEER-REVIEWED | Posted: 2 December 2021 doi:10.20944/preprints202112.0037.v1

Applying the known constants, we obtain the following equation for d_3:

$$\left(0.000126 \cdot d_3^{2.9091}\right) + \left(0.110214 \cdot d_3^{1.4545}\right) = 180$$

Solving this equation numerically with binary search, the value of $d_3 \approx 77.86$ is defined. Using this value, the constant vectors Ψ and θ, and lastly the ratios of Eq. 11 the remaining link lengths can be defined:

$$d_2 = 0.000126 \cdot 77.86^{1.4545} = 62.17$$
$$d_1 = 180 - 77.86 - 62.17 = 39.97$$

In this case, the maximum $P_{\mathtt{net}}$ that can be achieved with the referred links occurs when the link lengths are $\mathbf{L}_{opt} = [39.97, 62.17, 77.86]m$. The corresponding $P_{\mathtt{net}}$ value is:

$$P_{\mathtt{opt}} = P(\mathbf{L}_{\mathtt{opt}}) = P_1(39.97) \cdot P_2(62.17) \cdot P_3(77.86) = 0.7806$$

With three links, we can still visualize the result with a 3D plot. Figure 5 shows the network PDR as a function of the lengths of the first two links, constrained by $d_1 + d_2 = L - d_3$. For each value of d_3 we obtain one 2-dimensional PDR curve similarly to the product curve in Figure 3. The black curve represents the one that contains the highest peak, which is the maximum network PDR, achieved when $d_3 = 77.86$m.

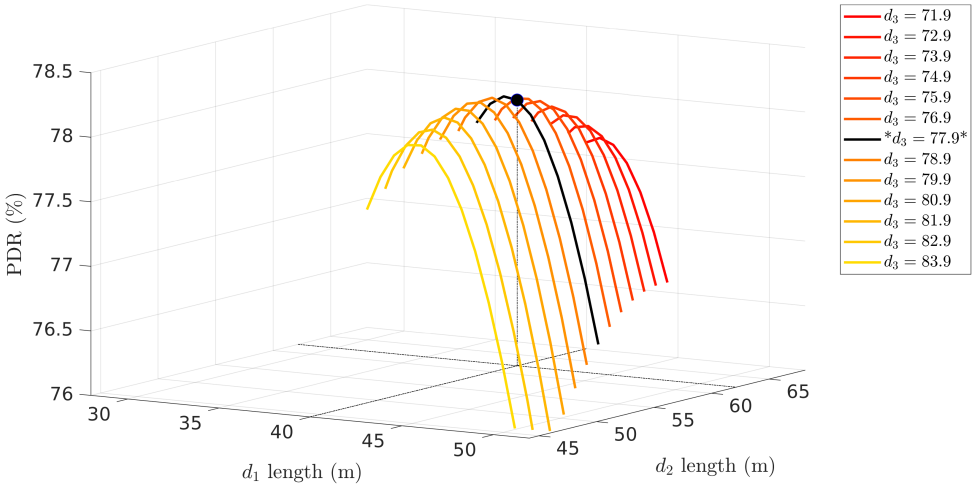

Figure 5. $P_{\mathtt{net}}$ - Network PDR as a function of the length of the three links. Maximum shown as black dot.

4.2. General performance assessment

There are benefits in optimizing the network PDR. In this section, a comparison is performed between the presented optimal solution and an intuitive solution consisting of placing the relays at equidistant intervals between the source and the sink (the baseline). To prove such claim, first, an example of a complex network with 7 links (6 relays) is presented to observe the improvement *optimal* versus *baseline* as a function of the total network length L. Second, a vast set of randomly generated link models is used to achieve a general empirical characterization of the performance improvement for different network lengths and number of links.

4.2.1. Performance improvement with 7 links

Consider a network with 7 links (6 relays) with different PDR models shown in Figure 6. Figure 7 shows the optimal positions of the six relays for different network length L (solid lines) together with the corresponding equidistant positions (dashed lines). Curiously, the curves also show what would be the path of all relay nodes in case

Preprints (www.preprints.org) | NOT PEER-REVIEWED | Posted: 2 December 2021 doi:10.20944/preprints202112.0037.v1

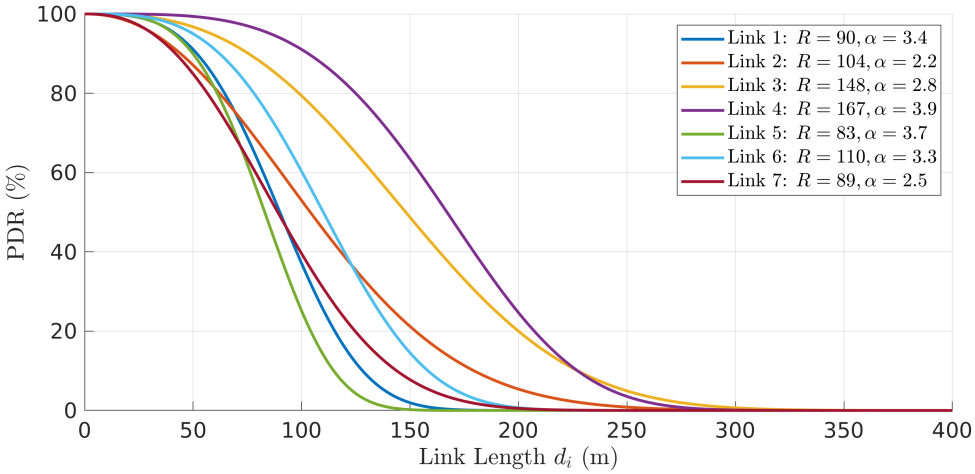

Figure 6. PDR models of 7 links as a function of link length d_i, where link i connects nodes i and $i+1$, $\forall i \in [1,7]$ (source is node 1 and sink is node n+1).

they kept their optimal / equidistant positions tightly while the source moved linearly away from the sink.

The absolute difference between optimal and equidistant positions increases non-linearly with network length. This can be better observed when plotting the relative positions of the relays concerning the fraction of the total network length instead of the absolute positions (Figure 8). The figure clearly shows that the optimal relative positions are not kept constant as the network length increases. This means that applying simple rules to maintain the relative position of each relay to their neighbors is not optimal as the network changes its overall length. In this case, the optimal positions have to be dynamically recomputed.

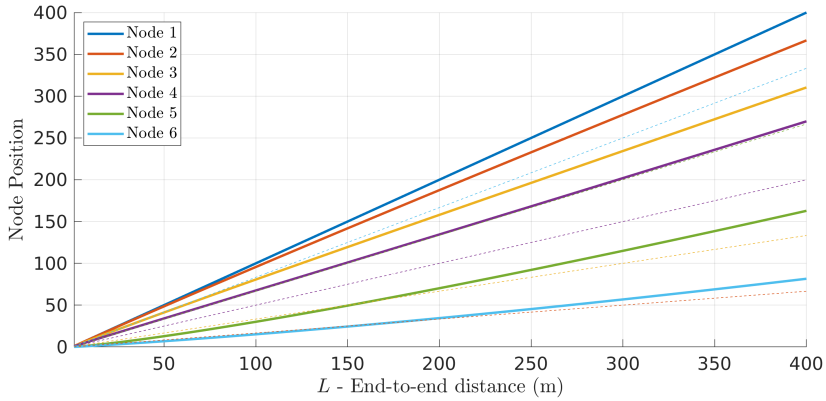

Figure 7. The optimal relay positions (solid lines) are different than the corresponding equidistant positions (dashed-lines). Their absolute differences increase (non-linearly) with network length L.

Looking now into the network PDR achieved with the optimal relays placement we can see a significant improvement when compared to what would be achieved with an equidistant placement instead, specially when the network increases its length. This is shown in Figure 9. In this particular example, when the network is 400m long, using the optimal solution increased the PDR by 15 percentage points, regarding equidistant placement. This represents a performance improvement of 35% (from $P = 42\%$ to $P = 57\%$). Note that the network (end-to-end) PDR when the relays are placed equidistantly, i.e., $P_{\texttt{equi}} = P_{\texttt{net}}(\mathbf{L}_{\texttt{equi}})$ with $\mathbf{L}_{\texttt{equi}} = \{d_i = L/n \; \forall d_i \in [1,n]\}$, can be computed using Eq. 16.

$$P_{\texttt{equi}} = P_{\texttt{net}}(\mathbf{L}_{\texttt{equi}}) = \prod_{i=1}^{n} P_i(L/n) \tag{16}$$

Preprints (www.preprints.org) | NOT PEER-REVIEWED | Posted: 2 December 2021 doi:10.20944/preprints202112.0037.v1

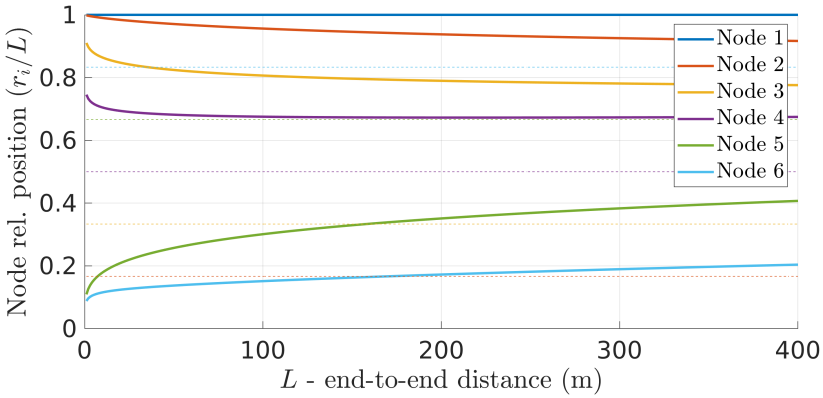

Figure 8. The relative positions of the relays as fractions of the total network length change with the network length itself.

The performance improvement, in network PDR, as a function of the network length L is shown in Figure 10. In particular, we show the relative PDR gain Φ - Eq. 17 - represents the additional PDR obtained with the optimal relay positioning relative to the network PDR obtained with equidistant relays.

$$\Phi = \frac{P_{\mathtt{opt}}}{P_{\mathtt{equi}}} - 1 = \frac{P_{\mathtt{net}}(\mathbf{L}_{\mathtt{opt}})}{P_{\mathtt{net}}(\mathbf{L}_{\mathtt{equi}})} - 1 \tag{17}$$

Figure 10 highlights the growing PDR improvement with growing network length. As we will see further on, this behavior is observed with any number of relays in the network. Increasing the number of relays significantly decreases the average length of the links, which also increases the end-to-end network PDR. However, more relays increase network delay. In general, we would be interested in using the least number of relays possible, which implies operating the network in the PDR region in which the PDR starts to drop. This is also the region where the optimal relay placement starts to make a difference, highlighting the relevance of this work.

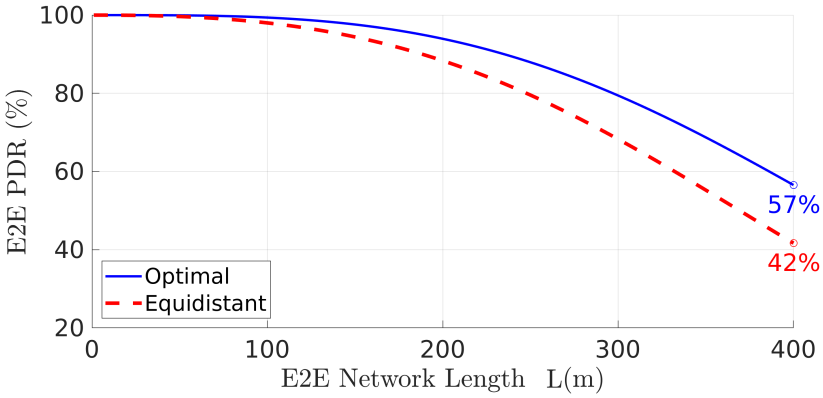

Figure 9. PDR $P_{\mathtt{net}}$ improves significantly when the optimal placement is used instead of equidistant positions, specially for larger network lengths.

4.2.2. General characterization with random links

To find a general characterization of the PDR improvement that can be achieved with the optimal relay placement, we generated 10000 random networks with random link models, varying number of relays and network length and observed the PDR gain Φ as defined in Eq. 17.

We started by generating a vast pool of links, where each link is generated with a random pair (R, α), taken uniformly from $R \in [80, 180]$ and $\alpha \in [2.1, 4.2]$, ranges that we observed in practice. The PDR link models are shown in Figure 11.

Preprints (www.preprints.org) | NOT PEER-REVIEWED | Posted: 2 December 2021 doi:10.20944/preprints202112.0037.v1

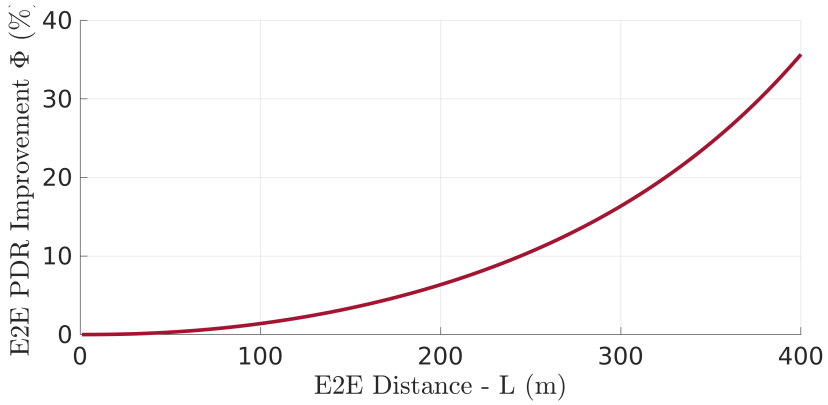

Figure 10. PDR $P_{\mathtt{net}}$ relative gain (Φ) using the optimal placement with respect to equidistant positioning.

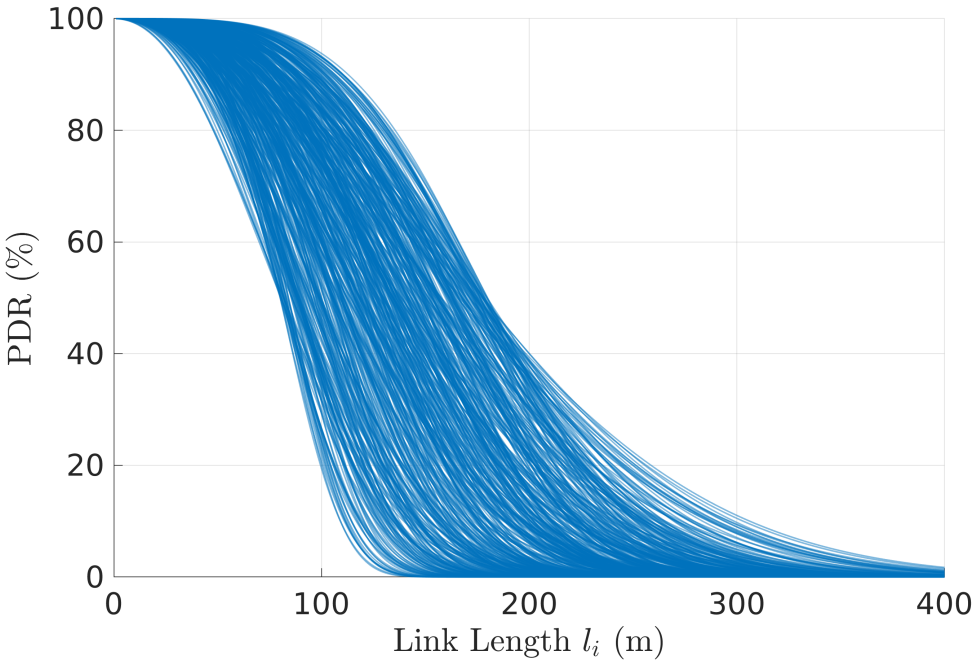

Figure 11. Pool of link PDR models (R, α) used for the general performance characterization ($R \in [80, 180]$ and $\alpha \in [2.1, 4.2]$).

Figure 12 shows the network PDR gain as a function of the number of links (equals the number of relays plus one) and network length in 10000 scenarios. Each scenario uses a random set of links (link models) generated from our pool. The scenarios are grouped per number of links and averaged. The curves represented in the figure are the average curves for all the scenarios generated with each number of links.

For a given distance, a lower number of links means the average length of each link is longer, thus the overall PDR is generally reduced. In these cases, the optimal placement has a strong impact. Moreover, lower number of links also reveals a faster increase in the optimal placement PDR gain, which comes together with an implicitly faster degradation of the network PDR. This shows that smaller networks (less relays) are more sensitive to the positioning of the relays.

In general terms, as expected, we will observe that the improvement depends on the asymmetry of the links. On the other hand, if all links have the same characteristics, the optimal solution is the equidistant solution and there is no performance improvement.

Preprints (www.preprints.org) | NOT PEER-REVIEWED | Posted: 2 December 2021 doi:10.20944/preprints202112.0037.v1

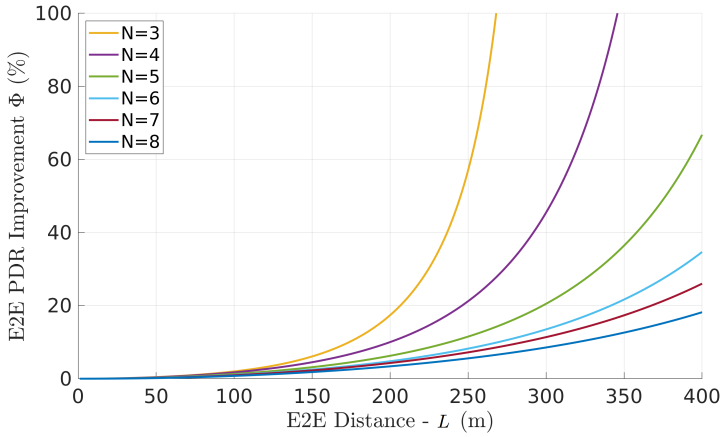

Figure 12. Average network PDR gain Φ (optimal relative to equidistant relay placement) with random link models, as a function of the number of links and network length L.

5. Deploying the Optimal Relay Placement

The previous sections gave us, already, good indications of the requirements for operating such a sensing network as well as the benefits that we can expect to achieve. However, to put in practice such a solution we need a deployment strategy that allows operating the relays network to reach the optimal relays positions. In this section we consider two possible approaches, centralized and distributed, which we explain and compare, next.

5.1. Centralized network control

In this approach, the control architecture relies essentially on the base station, taking advantage of its sink role in the network and potentially higher computing capacity. This approach consists of two phases, a trigger phase, for example, based on tracking the position of the source node and/or the PDR models of the links. This tracking can also be either centralized or distributed. For consistency with this deployment approach, we assume the source node reports its position and the relays report their PDR measurements from the links they receive from with adequate intervals, e.g. every x seconds. Then the ground station updates its knowledge of the source position and the PDR link models and checks whether these change beyond predefined thresholds and, if so, generates a re-positioning event. If this tracking is distributed, the event detection is left to the UAVs that communicate the re-positioning events, when they occur, to the base station. A re-positioning event initiates the second phase, in which the ground station computes new optimal relay positions and transmits them upstream to the relays as waypoints.

One important aspect is that the total time to reconfigure the network and have the relays taking their optimal positions is dominated by the physics of the UAVs - motion and control. Naturally, this time depends on the distance between the relays starting and target points. For long networks, this can be several meters apart, taking several seconds to re-position the relays.

Other properties of this approach include the concentration of the computational effort to update the links PDR models and compute the optimal relay positions. Naturally, this extra complexity of the ground station is paired with a corresponding simplification of the computational requirements of the UAVs. This solution also implies extra communications downstream that must be always running, even in periods in which the source sensing stream may not be needed, as during autonomous source replacement maneuvers. If a distributed event-detection is used, this burden on constant communication is alleviated, but the event communication must be carried out with reliability mechanisms in place.

Preprints (www.preprints.org) | NOT PEER-REVIEWED | Posted: 2 December 2021 doi:10.20944/preprints202112.0037.v1

Finally, this solution falls in the class of event-triggered systems. In the absence of changes in the network, no re-positioning event would be generated and no new way-points would be sent to the relay UAVs. Given its simplicity of deployment, we will use this approach as baseline when comparing with the distributed approach that we describe next.

5.2. Distributed network control

In a distributed context, each UAV places itself optimally, solely with local knowledge. This means that it tracks the positions of its neighbors and the PDR of the links it is engaged with, and computes its own optimal position, only, considering a two-links case. Thus, the computational effort required to the UAVs is naturally higher than with the centralized approach, but it is limited, too, and does not depend on the number of relays used. The ground station, conversely, is not involved in the re-positioning of the relays, which simplifies its design.

However, the optimization process must be executed iteratively since the optimal positions computed in each step are just locally optimal. Thus, we have to show that the sequence of local optimal positions converges to the global optimal placements generated by the centralized approach. We will address this issue later in this section.

Overall, this solution falls on the class of time-triggered systems in which the positions of the relays are being periodically tracked and adjusted by all relays, in parallel, so as the adjustment of the PDR models of their links. Thus, changes in relay positions or source position, or variations in links PDR can be compensated readily in an organic fashion, without engaging in global mechanisms. Thus, the line network of relays autonomously tracks its optimal configuration.

5.2.1. Implementing the distributed control method

The implementation of the distributed control method is rather simple, too. In a network with n links we have n UAVs of which 1 to $n-1$ are relays. All network nodes regularly share their position with their neighbors, for example, 3D coordinates in a ENU (East-North-Up) fixed frame. Consider the relay i and its position r_i. For simplicity, consider node positions are one-dimensional with origin defined at the Sink. Its neighbors are the upstream node $i-1$, with which it shares link $i-1$ and which is in position r_{i-1}, and the downstream node $i+1$, with which it shares link i and which is in position r_{i+1}. The PDR models of both links are also known by relay i, namely (R_{i-1}, α_{i-1}) and (R_i, α_i).

Knowing the neighbors positions (r_{i-11}, r_{i+1}) as well as its own (r_i), relay i can compute the lengths of both links, l_{i-1} and l_i. With this information, it can apply the optimization method described in the previous section, applied to the simple two links case as in Section 4.1.1, to compute its local optimal way-point. This process is repeated with an adequate period T as described in the following listing. While all relays from 2 to n execute this process, the source UAV and the ground station (sink) simply answer the request for position issued by their neighbor relays. The behaviour just described for relay i is summarized in the pseudo-algorithm below.

loop (every T)
  $\{r_{i-1}, r_i, r_{i+1}\}$ = REQUESTPOSITION(nodes=$\{i-1, i+1\}$) ▷ Obtain position of neighbors
  r_i^{opt} = GETOPTPOSITION($\{r_{i-1}, r_i, r_{i+1}\}$, $\{(R_{i-1}, \alpha_{i-1}), (R_i, \alpha_i)\}$)
  SETDRONETARGET(r_i^{opt}) ▷ Set waypoint for the local optimal position
end loop
procedure GETOPTPOSITION($\{r_a, r_b\}$, $\{(R_a, \alpha_a), (R_b, \alpha_b)\}$)
  $\{\Psi_{a,b}, \theta_{a,b}\} \leftarrow f_{Eq13}(\{(R_a, \alpha_a), (R_b, \alpha_b)\})$ ▷ cf. Eq.13
  $L \leftarrow ||r_a - r_b||$ ▷ Current length of this network portion
  $d_b \leftarrow \{x \in \mathcal{R} : \Psi_{a,b} \cdot x^{\theta_{a,b}} + x = L\}$
  $d_a \leftarrow L - d_b$ ▷ Compute optimal link lengths

Preprints (www.preprints.org) | NOT PEER-REVIEWED | Posted: 2 December 2021 doi:10.20944/preprints202112.0037.v1

$r_i \leftarrow r_b + d_b$ ▷ Compute optimal position
return r_i
end procedure

5.2.2. Example

Figure 13 shows the same case with four links ($n = 4$), thus three relays, where the link PDR models were generated randomly ($R = \{154, 177, 98, 108, 178\}, \alpha = \{2.53, 3.38, 2.38, 2.59\}$). The source node is fixed at $r_1 = L = 400$m from the base station and the initial positions of the three relays are equidistant ($r_4 = 100$m, $r_3 = 200$m and $r_2 = 300$m, respectively). The horizontal axis shows the number of iterations of the algorithm, repeated with a period of $T = 1$s (top) and $T = 5$s (bottom). The vertical axis represents the position of each relay r_i along the line between source and base station.

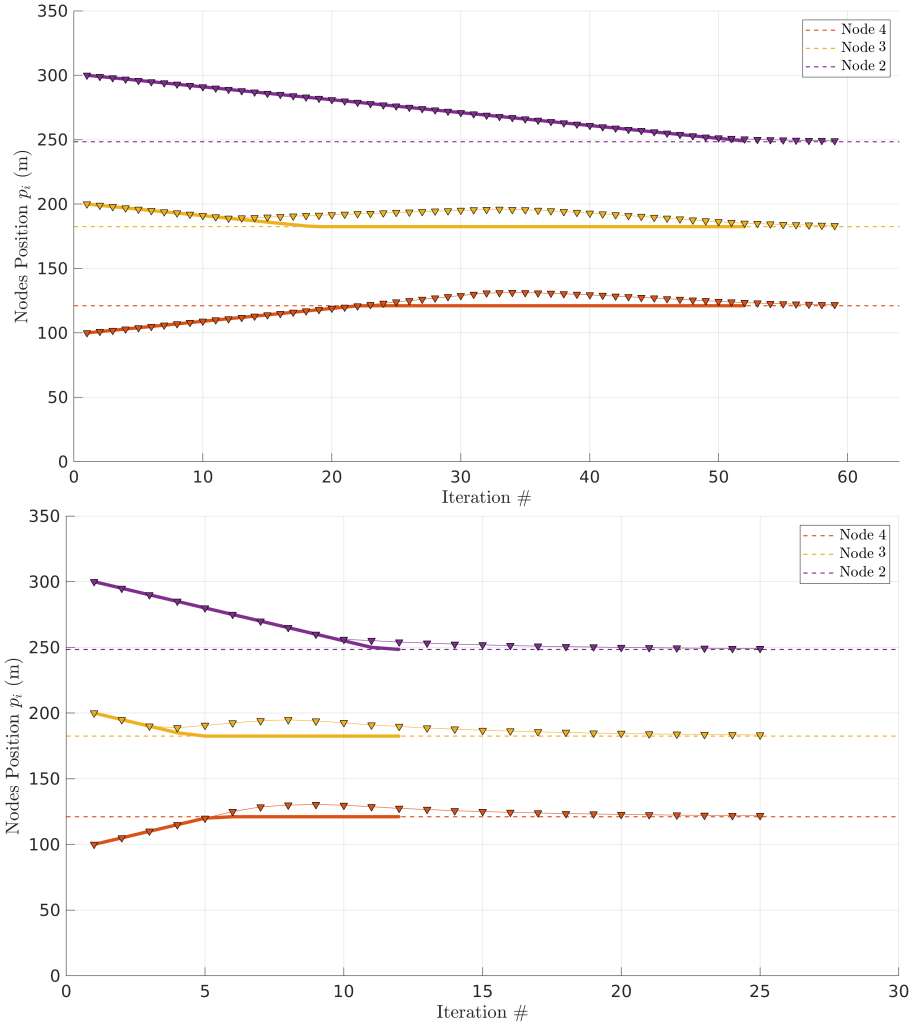

Figure 13. Nodes converging to their optimal position. Triangles represent relay positions every step of the distributed approach. Solid lines show the evolution of a centralized approach. (Iterations with T=1s (Top) and T=5s (Bottom); note the different horizontal scales)

The dashed lines represent the optimal positions for all the relays. The solid lines show the relays movement when the global optimal positions are computed at once by the ground station in a centralized approach. In this case, the relay UAVs are assigned way-points corresponding to their optimal positions and move directly to those points at constant cruise speed (1m/s). Once they reach the optimal positions they stay there.

The triangles show the relays behavior running our distributed approach in which the global optimal locations are not known a priori. We also assume the vehicles move

Preprints (www.preprints.org) | NOT PEER-REVIEWED | Posted: 2 December 2021 doi:10.20944/preprints202112.0037.v1

at the same cruise speed of 1m/s. In this case, the relays share position information with their neighbors every iteration ($T = 1$s or $T = 5$s).

Observing Figure 13 we can see that the centralized approach, despite the immediate computation of the optimal positions, takes 52s to converge. We define convergence as the situation in which all relays are at less than 1 meter from their optimal positions. Curiously, the distributed approach generates sets of local optimal positions to drive the relays, but for some relays and in certain periods, the local optimal positions fall on the UAVs trajectory resulting from the centralized approach. Eventually, there is some bounded divergence for some time, but the distributed approach converges to the global optimal positions. With $T = 1$s, it takes $\sim$ 59s to converge. This time increases to $\sim$ 125s with $T = 5$s.

5.2.3. Convergence of distributed control

At this point, we have not achieved a formal proof of convergence, yet, for the distributed approach. Thus, we tested the convergence hypothesis empirically using 10000 random scenarios from the same pool of random link PDR models (R, α) used in Section 4.2.2. In each scenario we compare the time (and track the number of iterations) necessary for the centralized and distributed approaches to converge. We consider two cases with different periods ($T \in \{1, 5\}$s).

Figure 14 shows the histograms of the ratios of the time taken by the distributed approach to converge over the time taken by the centralized approach. We can observe that larger periods take significantly longer to converge. The average ratio grows from $\sim$ 1.4 to $\sim$ 4 with $T = 1$s and $T = 5$s, respectively. Moreover, note that the network is insensitive to changes in positions or link PDR models during each period. Thus, longer periods also generate additional latency in reacting to such changes.

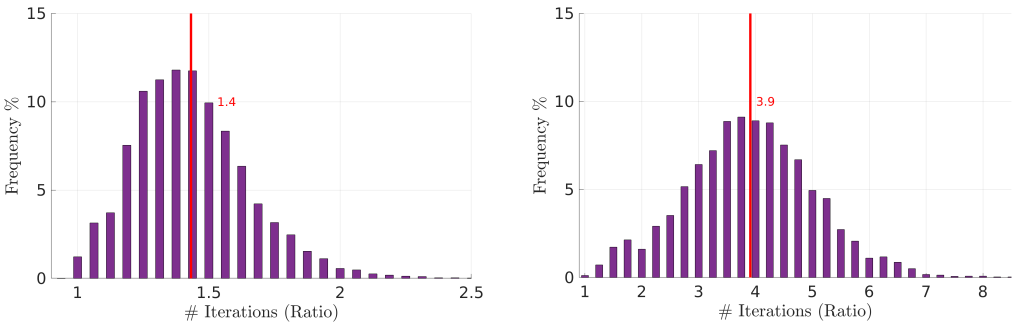

Figure 14. Distribution of the ratio distributed over centralized convergence time for different values of T. (Left: $T = 1$s; Right: $T = 5$s)

Naturally, sufficiently longer periods will necessarily create instability and prevent the distributed approach from converging. However, we have tried with $T = 15$s and still achieved convergence, despite taking, on average, $\sim$ 8 times the time taken by the centralized approach. On the other hand, setting too short periods creates additional communication and computing overhead that may turn the network inoperable. Thus, an adequate compromise must be set, considering the desired reactivity to changes, speed of convergence and communications and computational overhead. Note. however, that the overhead implied by the distributed network control method is low, consisting of one short packet exchange with each neighbor to get their positions and one optimal position computation per iteration (every T). In such circumstances, we believe that $T = 1$s is a suitable choice.

5.3. On tracking the links PDR models

The deployment methods referred before assume the links PDR model is known. However, this information is typically unknown *a-priori*. The PDR of each link depends on the area of operation, whether there are obstacles in the area or alien transmitters

Preprints (www.preprints.org) | NOT PEER-REVIEWED | Posted: 2 December 2021 doi:10.20944/preprints202112.0037.v1

generating interference, as well as on specific features of the nodes involved, such as their antennas, sensitivity and noise resilience. Consequently, the links PDR must be measured at run-time so as the estimation of the PDR model parameters (R, α).

This is, in itself, a topic of research and we will not explore it in detail in this work. However, a preliminary strategy has been proposed in [4] and we explain here the basis of its operation. Essentially, the network of UAVs is configured, i.e., defining the number of relays, according to preliminary approximate knowledge of the communication range of the UAVs, possibly taking a conservative approach. Then, the network is deployed at once, with the UAVs being launched in sequence, with the source UAV heading to its initial target and the relay UAVs moving to an equidistant placement between source and sink. This initial travel will take a few seconds during which the UAV will already exchange a few hundreds of packets[3]. All packets are piggybacked with position information and a sequence number. This allows all receivers to build PDR statistics as a function of link distance, for example, every second, allowing to identify the model of each link PDR[4].

Once the UAVs arrive at their equidistant positions, they will initiate the optimization process to update their positions for maximal PDR. Nevertheless, the PDR measurement and model estimation will continue, always. This process requires a small adaptation of the *RequestPosition* procedure in the pseudo-code in Section 5.2.1). In fact, the position from the upstream UAV comes embedded in the sensing stream, thus there is no need to ask for it. Moreover, each relay UAV can locally build the PDR model of the upstream link, too. Consequently, the referred procedure just needs to ask the position of the downstream UAV as well as the PDR model of the downstream link to gather the data needed to execute the distributed network control.

6. Conclusion

Aerial sensing with multirotor UAVs, in particular, has become common for a myriad of applications including for remote inspection of difficult to access structures in large industrial plants. In this paper we addressed the case of extending the range of operation of such a UAV adding aerial relaying support. However, the placement of the relay UAVs is crucial for the end-to-end network performance, notably in what concerns the PDR. We tackled the non-trivial issue of finding the optimal positions that maximize the network PDR in the presence of asymmetrical links. Resorting to simulation, we characterized the average network PDR improvement that can be expected considering a pool of random but realistic link PDR models and how such improvement varies with network length and number of links (or relays). Finally, we addressed the deployment method of the proposed optimization so that the network can be operated in practice. We proposed a fully distributed approach that presents reduced overhead and keeps the relays in optimal positions in an organic manner. With the same pool of random links, we generated 10000 random networks and executed this distributed approach. When iterated with a period of 1s, we found that it converges from an equidistant placement to the optimal positions, on average, in 1.4 the time taken by a centralized method, but without any global coordination. On the other hand, the formal proof of convergence and the online estimation of the links PDR model were essentially left for future work.

Author Contributions: "Conceptualization, L. Pinto and L. Almeida; methodology, L. Pinto and L. Almeida; software, L. Pinto.; validation, L. Pinto and L. Almeida; formal analysis, L. Pinto; investigation, L. Pinto; resources, L. Pinto and L. Almeida; data curation, L. Pinto; writing—original draft preparation, L. Pinto and L. Almeida; writing—review and editing, L. Almeida; visualization, L. Pinto; supervision, L. Almeida; project administration, L. Almeida; funding acquisition, L. Almeida. All authors have read and agreed to the published version of the manuscript.", please turn to the CRediT taxonomy for the term explanation.

[3] The transmission of the sensing stream is bandwidth intensive, easily reaching 50 to 100 packet/s

[4] Since the UAVs are moving, the PDR statistics will consider an average distance during the period in which the packets were collected.

Funding: Please add: "This research was funded by Fundação para a Ciência e a Tecnologia, Portugal, under grant UIDB/04234/2020 - CISTER Research Unit."

Data Availability Statement: In this section, please provide details regarding where data supporting reported results can be found, including links to publicly archived datasets analyzed or generated during the study. Please refer to suggested Data Availability Statements in section "MDPI Research Data Policies" . You might choose to exclude this statement if the study did not report any data.

Conflicts of Interest: "The authors declare no conflict of interest." "The funders had no role in the design of the study; in the collection, analyses, or interpretation of data; in the writing of the manuscript, or in the decision to publish the results".

References

1. Nikolic, J.; Burri, M.; Rehder, J.; Leutenegger, S.; Huerzeler, C.; Siegwart, R. A UAV system for inspection of industrial facilities. 2013 IEEE Aerospace Conference (AeroConf), 2013, pp. 1–8. doi:10.1109/AERO.2013.6496959.
2. Pinto, L.R.; Moreira, A.; Almeida, L.; Rowe, A. Characterizing Multihop Aerial Networks of COTS Multirotors. *IEEE Transactions on Industrial Informatics* **2017**, *13*, 898–906. doi:10.1109/TII.2017.2668439.
3. Pinto, L.R.; Almeida, L.; Alizadeh, H.; Rowe, A. Aerial Video Stream over Multi-hop Using Adaptive TDMA Slots. 2017 IEEE Real-Time Systems Symposium (RTSS), 2017b, pp. 157–166. doi:10.1109/RTSS.2017.00022.
4. Pinto, L.R.; Almeida, L.; Rowe, A. Balancing Packet Delivery to Improve End-to-End Multihop Aerial Video Streaming. ROBOT 2017: Third Iberian Robotics Conference; Ollero, A.; Sanfeliu, A.; Montano, L.; Lau, N.; Cardeira, C., Eds.; Springer International Publishing: Cham, 2018; pp. 807–819.
5. Forster, C.; Lynen, S.; Kneip, L.; Scaramuzza, D. Collaborative monocular SLAM with multiple Micro Aerial Vehicles. 2013 IEEE/RSJ International Conference on Intelligent Robots and Systems, 2013, pp. 3962–3970. doi:10.1109/IROS.2013.6696923.
6. Pinto, L.R.; Vale, A.; Brouwer, Y.; Borbinha, J.; Corisco, J.; Ventura, R.; Silva, A.M.; Mourato, A.; Marques, G.; Romanets, Y.; Sargento, S.; Gonçalves, B. Radiological Scouting, Monitoring and Inspection Using Drones. *Sensors* **2021**, *21*. doi:10.3390/s21093143.
7. Asadpour, M.; Giustiniano, D.; Hummel, K.A.; Heimlicher, S.; Egli, S. Now or later?: Delaying Data Transfer in Time-critical Aerial Communication. Proc. Ninth ACM Conf. Emerg. Netw. Exp. Technol. (CoNEXT); ACM Press: Santa Barbara, CA, USA, 2013; pp. 127–132.
8. Holland, G.; Vaidya, N.; Bahl, P. A Rate-adaptive MAC Protocol for multi-Hop Wireless Networks. Proceedings of the 7th Annual International Conference on Mobile Computing and Networking; ACM: New York, NY, USA, 2001; MobiCom '01, pp. 236–251. doi:10.1145/381677.381700.
9. Goddemeier, N.; Daniel, K.; Wietfeld, C. Role-Based Connectivity Management with Realistic Air-to-Ground Channels for Cooperative UAVs. *IEEE Journal on Selected Areas in Communications* **2012**, *30*, 951–963. doi:10.1109/JSAC.2012.120610.
10. Zhao, J.; Govindan, R. Understanding packet delivery performance in dense wireless sensor networks. Proc. First Int. Conf. Embed. Networked Sens. Syst. (SenSys); ACM Press: Los Angeles, CA, USA, 2003; p. 1.
11. Jia, F.; Shi, Q.; Zhou, G.m.; Mo, L.f. Packet Delivery Performance in Dense Wireless Sensor Networks. Proc. Int. Conf. Multimed. Technol. (ICMT); IEEE: Ningbo, China, 2010; pp. 1–4.
12. Bohm, A.; Lidstrom, K.; Jonsson, M.; Larsson, T. Evaluating CALM M5-based vehicle-to-vehicle communication in various road settings through field trials. Proc. IEEE Local Comput. Netw. Conf. (LCN); IEEE: Denver, CO, 2010; pp. 613–620.
13. Lindhe, M.; Johansson, K. Using robot mobility to exploit multipath fading. *IEEE Wirel. Commun.* **2009**, *16*, 30–37.
14. Henkel, D.; Brown, T.X. Delay-tolerant communication using mobile robotic helper nodes. Proc. Int. Symp. Model. Optim. Mobile, Ad Hoc, Wirel. Networks Work. (WiOPT); IEEE: Berlin, Germany, 2008; pp. 657–666.
15. Sicignano, D.; Tardioli, D.; Cabrero, S.; Villarroel, J.L. Real-time wireless multi-hop protocol in underground voice communication. *Ad Hoc Networks* **2013**, *11*, 1484–1496. Special Issue on Wireless Communications and Networking in Challenged Environments.

 doi:10.20944/preprints202112.0037.v1

16. Rizzo, C.; Tardioli, D.; Sicignano, D.; Riazuelo, L.; Villarroel, J.L.; Montano, L. Signal-based deployment planning for robot teams in tunnel-like fading environments. *Int. J. Rob. Res.* **2013**, *32*, 1381–1397.

 doi:10.20944/preprints202112.0037.v1